On the Inoperativeness of the ESIPT Process in the Emission of 1-Hydroxy-2-acetonaphthone: A Reappraisal

J. Catalán* and J. L. G. de Paz

Departamento de Química Física Aplicada, Universidad Autónoma, C-II-203, Cantoblanco, 28049 Madrid, Spain

Received: August 3, 2007; In Final Form: November 14, 2007

For a molecule which contains an intramolecular hydrogen bond (IMHB) in its chemical structure to undergo an excited singlet intramolecular proton transfer (ESIPT) process, on photoexcitation, there must occur a simultaneous increase, in a substantial manner, in the acidity of the proton donor and the basicity of the proton acceptor forming the IMHB [*J. Am. Chem. Soc.* **2001**, *123*, 11940]. For the reason that those changes occur on photoexcitation of the 2-hydroxyacetophenone but not for 1-hydroxy-acetonaphthone, one draws the conclusion that, while ESIPT is operative in the $1(\pi,\pi^*)^1$ electronic state of the monocyclic compound 2-hydroxyacetophenone, it is not operative in its bicyclic homolog 1-hydroxy-2-acetonaphthone. We have shown the photophysics of 1-hydroxy-2-acetonaphthone in its first excited electronic state to be governed by two stable, easily reconverted enol structures, the presence of which causes the peaks in the free-jet fluorescence excitation spectrum for the compound to split into two of similar strength. In this paper, we rationalize photophysical evidence for 1-hydroxy-2-acetonaphthone obtained by femtosecond spectroscopy over the past 13 years in the light of existing photophysical patterns based on steady-state spectra for the compound [*J. Am. Chem. Soc*. **1993**, *115*, 4321].

Introduction

Early studies on the fluorescence of 1-hydroxy-2-acetonaphthone (HAN, Scheme 1) in the gas and solid phases and also in highly dilute solutions in cyclohexane, methanol, and DMSO at 298 and 77 K[1,2] showed unexpected photophysical properties for this chromophore. Although HAN possesses a strong intramolecular hydrogen bond (IMHB),[2] its fluorescence is inconsistent with the existence of a first excited singlet state intramolecular proton transfer (ESIPT) and yet the compound is more photostable than 5-methyl-2-hydroxyphenylbenzotriazole (TIN-P), which is currently held as a prototype of photostability.[2]

The structure and photophysical behavior of HAN are special in some respects, namely,[2] (1) the IMHB is so strong that it cannot be broken even by dissolution in strong acidic or basic solvents such MeOH or DMSO, respectively, and (2) however, electronic excitation seemingly does not trigger ESIPT via the IMHB since (a) the emission at 298 K, which peaks at approximately 470 nm, exhibits acceptable mirror symmetry with the first absorption band for the compound; (b) the expected emission for an ESIPT process, which is typically assigned a Stokes shift of approximately 11 000 cm^{-1}, has never been detected for this compound in any studied medium; and (c) the fluorescence quantum yield of HAN changes very little upon deuteration of its phenolic proton.

By contrast, the photophysics of the HAN monocyclic homolog 1-hydroxy-2-acetophenone (HAP, Scheme 1) and other salicyl compounds containing an IMHB is controlled by efficient ESIPT; also these compounds exhibit fluorescence with a Stokes shift of approximately 11 000 cm^{-1}, no mirror symmetry between their fluorescence and first absorption bands, and a quantum yield that changes upon deuteration of the phenolic proton.

SCHEME 1: Molecular Structures of HAN(1-hydroxy-2-acetonaphthone), HAP(2-hydroxyacetophenone), and HBA(salicyladehyde), and Atom Numbering Scheme Used

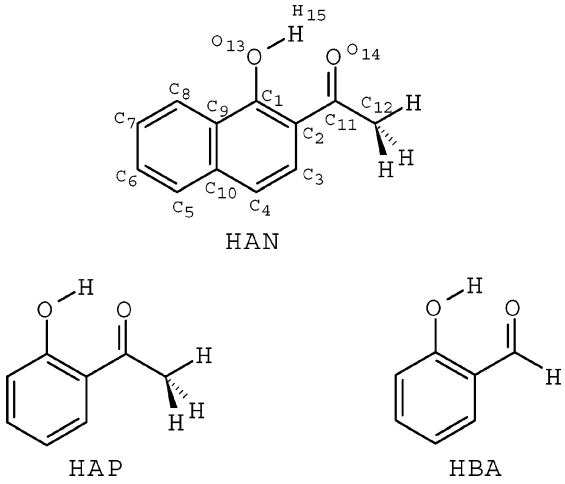

In 1993, Douhal et al.[3] examined fluorescence excitation and dispersed emission spectra for HAN obtained under free-jet expansion conditions and concluded that the fluorescence of this chromophore has a dual nature (viz., that it actually consists of two fluorescence emissions: one, which they called "short wavelength fluorescence", is highly structured and has a 0−0 component matching that of its absorption; and the other comprising the emission beyond 2200 cm^{-1}, which they called "long wavelength fluorescence" and is stronger and more diffuse). Consistent with the assignment based on the dispersed emission and excitation spectra, they concluded that "the

* Corresponding author. E-mail: javier.catalan@uam.es.

10.1021/jp076228r CCC: $40.75
Published on Web 01/15/2008

SCHEME 2: Reported Structures for the Keto Form of HAN

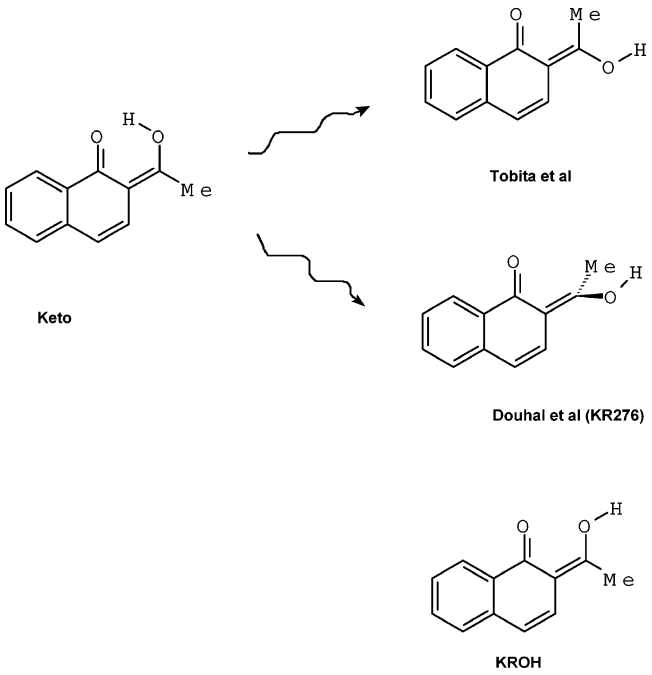

Tobita et al. ref 8; Douhal et al. refs 6, 10−15; Kroh this work. The curly arrows represent a nonradiative process.

fluorescence excitation and structured short wavelength emission of HAN have an approximate mirror image. It may be deduced that the states involved in the $S_0 \leftrightarrow S_1$ transitions are reasonably similar in bonding and electron distribution and can be attributed to the normal enol form of HAN" and also that "the excitation spectrum of HAN is composed of narrow bands with an intense 0−0 transition and is thus typical of an allowed transition between two states with moderately displaced equilibrium geometries". According to these authors, the long wavelength fluorescence was produced by the tautomeric keto conformer resulting from an ESIPT process, and the short wavelength fluorescence was purduced by the normal (enol) conformer resulting from electronic photoexcitation.

Douhal et al.[3] interpreted the unique photophysical behavior of HAN by assuming the curve controlling proton transfer in the first excited singlet state to be a double-minimum curve where both minima have very similar energies and exhibit tunneling. In 1996, Douhal et al.[4] justified the presence of two structured emissions in the fluorescence spectrum of HAN by using a diagram where the potential energy curves for both the ground electronic state and the first excited singlet were of the double-minimum type and thus consistent with two electronic transitions for the emission between the corresponding enol and keto structures.

In previous work, we showed the keto tautomer of HAN in the ground electronic state to be unstable.[5] This finding was subsequently confirmed by other authors[6,7] and led Tobita et al.[8] to use an additional structure, one which they assumed to be the result of ESIPT in the compound, in order to interpret their own transient absorption spectra. These authors assumed the keto form produced by ESIPT to undergo reconversion in its S_1 state by rotation about its protonated keto group (see the Tobita form in Scheme 2), followed by fast internal conversion to S_0 (the structure inferred from their transient absorption spectrum). They also showed that obtaining such a structure required the presence of an alcohol and triethylamine in the HAN solution. Subsequently, Lu et al.[9] used femtosecond time-resolved multiphoton ionization spectroscopy to study HAN in the gas phase and found the compound to exhibit a biexponential decay in its S_1 state which they ascribed to the presence of an enol form and a keto form in equilibrium, the keto tautomer crossing a very low-energy barrier (ca. 0.95 kcal/mol) at S_1; however, they omitted the presence of a rotated keto form generated from the keto tautomer.

Owing to the fact that, in the ground electronic state, the keto form does not exhibit any energy minima,[5] Douhal et al.[6,10−15] assume the existence of another chemical structure that enables to explain the strong vibronic structure monitored for the so-called "long wavelength fluorescence". This new molecular structure must be generated from the electronically excited enol form and must exhibit minima in both the S_1 and the S_0 states. As it was previously reported by Tobita el al.,[8] Douhal et al. proposed the presence of a structure of the protonated keto group in which would be virtually normal to the naphthalene ring in the compound. They named such a structure KR*(276). These authors[12] compared the fluorescence of HAN in a molecular beam and in methylcyclohexane at 80 K and concluded that the peaks at 426 and 452 nm in the molecular beam spectrum were correlated with those at 460 and 485 nm observed in the spectrum in methylcyclohexane at 80 K; they assigned such peaks to emissions from two forms which they called K* and KR*, respectively. According to these authors, KR* is 6.23 kcal/mol more stable than the corresponding electronically excited enol form of the compound (see Figure 2 in reference 10); also, it strongly reduces the aromaticity of the compound in its ground electronic state. Therefore, this species must be highly unstable (about 22 kcal/mol based on Figure 2 in reference 10). Accordingly, the 0−0 component of the emission from KR*-(276) should fall in the region of 630 nm or be even more markedly red-shifted if the zero point correction is applied. In summary, emission from this structure can hardly be the origin of the emissive behavior of HAN as it departs markedly from existing experimental evidence for the compound.

By using time-resolved photoelectron spectroscopy with a sample of HAN excited at 355−370 nm, Lochbrunner et al.[16] obtained two photoionization bands which they assigned to the photoionization of the enol and keto forms of the compound in its S_1 state and calculated the splitting between their thresholds to be approximately 5.8 kcal/mol. Femtosecond time-resolved transient absorption experiments subsequently conducted by Lochbrunner et al.[17] revealed that the nuclear coordinates contributing to the reaction pathway beyond the Franck−Condon region where dominated by the H-chelate ring; their most surprising conclusion, however, was that, on the basis of Figure 1 in the previous reference, they assigned the fluorescence of HAN in cyclohexane to its keto form. On the basis of recent Raman spectroscopy results,[7] the vibrations of the excited enol form of HAN resulting in the greatest shifts are the stretching and in-plane deformation modes of the naphthalene ring and the conjugated carbonyl group; by contrast, the OH stretching mode exhibits no appreciable change.

Therefore, at least the short wavelength portion of the fluorescence of HAN appears to be due to the enol form produced by direct electronic excitation of the compound.[1−4] On the basis of nano- and femtosecond time-resolved spectroscopic evidence, it is also obvious that a new structure is rapidly produced from the directly excited enol form which has been identified with the excited keto form on no experimental grounds. Available spectroscopic evidence for HAN includes significant facts potentially useful with a view to clarify the following issues: (1) the doublet nature of the 0−0 component

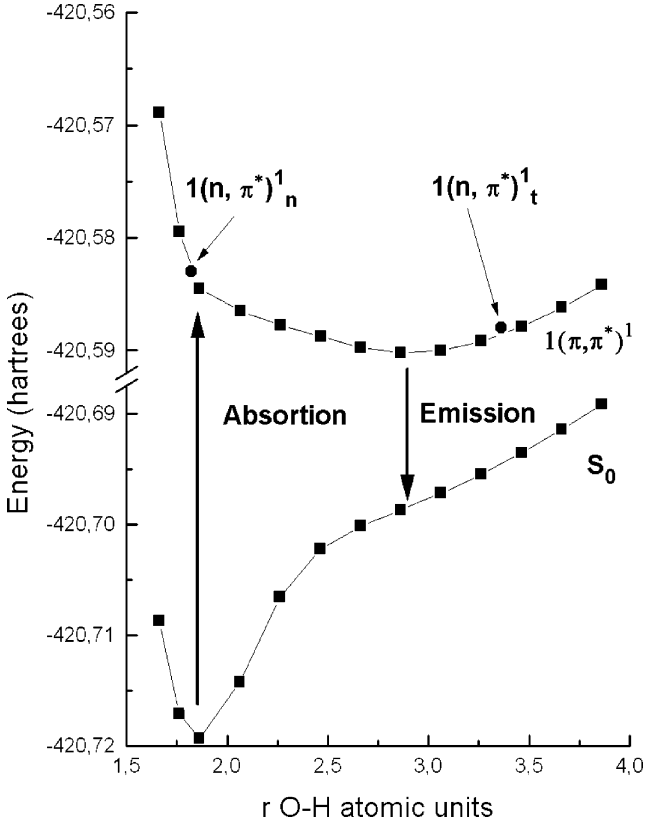

Figure 1. Potential energy profiles as a function O−H bond distance for the donor in the ground electronic state, S_0, and the S_1 (π,π^*) state in HBA. Stationary points were fully optimized under no constraint. All other points were calculated by freezing the O−H distance and fully optimizing the remaining geometrical parameters. The position of the $(n,\pi^*)^1$ state is indicated.

TABLE 1: Spectroscopic Data, in Nanometers, for HBA

electronic transition	TDDFT/B3LYP//TZVP this work[a]	RI-CC2/TZVP[46]	CASPT2/6-31G**[45]	expt
vertical ($S_0^n \rightarrow S_1(\pi,\pi^*)$)	315	303	332	328[b]
vertical ($S_1^t(\pi,\pi^*) \rightarrow S_0$)	466	521	515	492[c]
0−0 ($S_0^n \rightarrow S_1^t(\pi,\pi^*)$)	370	385[e]	406[e]	377[d]
0−0 ($S_0^n \rightarrow S_1^n(n,\pi^*)$)	348	359[e]		
0−0 ($S_0^n \rightarrow S_1^t(n,\pi^*)$)	362	405[e]		

[a] State energies and corresponding zero point energy corrections, in atomic units, as calculated for the molecular structures of HBA: ground state enol −420.719337, 0.115293; $1(\pi,\pi^*)^1_{keto}$ −420.590948, 0.110083; $1(n,\pi^*)^1_{enol}$ −420.583183, 0.110142; $1(n,\pi^*)^1_{keto}$ −420.588298, 0.110618. All structures possess C_s symmetry. [b] λ_{max} for the first absorption band in an Ar matrix at 12 K (see Figure 5 in reference 37). [c] The fluorescence maximum in Ar matrices at 22 K spanned the wavelength range 468−520 nm and peaked at 492 nm (see ref 37). [d] Evaluated from the maximum at 328 nm and the difference between the onsets of the photoelectronic spectra, which was estimated to be 0.5 eV by Lochbruner et al.[16,17] [e] ΔE value for each process as corrected for our calculated ZPE value.

of the $S_0 \leftrightarrow S_1$ transition in the excitation spectrum for HAN under free-jet expansion conditions, (2) the anomalous photophysical behavior of the compound upon deuteration of its phenolic proton, (3) the disparate ionization energy of the two forms present in the excited electronic state, (4) the energy of the $1(n,\pi^*)^1$ excited electronic state in these structures, and (5) the structure initially generated from the enol form that results from the absorption of light by the compound.

Clearly, if we can justify these issues and explain why the photophysical behavior of HAN departs from the well-established behavior of its monocyclic homolog 1-hydroxy-2-acetonaphthone (HAP), we will be able to acquire a much better understanding of the photophysics of such an interesting compound.

In this work, we used theoretical DFT and TDDFT calculations for the different species potentially involved in the photophysics of HAN and compared them with those for *o*-hydroxybenzaldehyde (HBA) and HAP. Also, we examined various experimental results in a search for potential changes in the envelope of the first absorption band and fluorescence emission of HAN dissolved in 2MB as the solution temperature is lowered. This data was used to justify or discard the presence of fluorescence emissions other than that produced by the normal form directly excited in the light absorption process.

Theoretical and Experimental Section

All computations for the ground electronic state were done within the framework of the density functional theory (DFT), and those for excited electronic states were done in the light of the time dependent density functional theory (TDDFT), using the Turbomole 5.25 and 5.8 software packages,[18] which were originally developed by the Quantum Chemistry Group of the University of Karlsruhe (Germany), in both cases. Full geometry optimization of ground electronic states and first excited $(\pi,\pi^*)^1$ and $1(n,\pi^*)$ states was done by using the Becke three-parameter hybrid functional (B3)[19,20] with the expression of Lee, Yang and Parr (LYP)[21] for nonlocal correlation (B3LYP) as implemented in Turbomole.[22] We chose to use the TZVP basis set[23,24] for compatibility with previous studies of our group in this field and also on the grounds of the system size. Excited states were studied at the TDDFT level[25] as implemented in Turbomole.[26−29] Minima were characterized by all-real vibrational frequencies. Previous studies had shown this methodology to be accurate in photoexcited molecules.[7,9,30] The doublet states involved in the electronic excitation of the minimum-energy structures in the first excited singlet state of the compound were also studied.

The 0−0 components of the $S_0 \leftrightarrow S_n$ electronic transitions were determined from the fully optimized geometries of the different states, with correction for the zero point energy (ZPE) as computed from the calculated numerical vibrational frequencies for the compound using Turbomole.

UV−visible spectra were recorded on a Cary-5 spectrophotometer furnished with Suprasil quartz cells of 1 cm light path. Spectroscopic emission measurements were made in Suprasil quartz cylindrical cells of 1 cm light path. Corrected fluorescence spectra were obtained on a calibrated Aminco−Bowman AB2 spectrofluorimeter. The sample temperature was controlled by using an Oxford DN1704 cryostat equipped with an ITC4 controller interfaced to the spectrophotometer. The cryostat was purged with dried nitrogen 99.99% pure.

1-Hydroxy-2-acetonaphthone (HAN) was obtained in 99% purity from Aldrich. The samples consisted of freshly made solutions containing approximately 10^{-5} M HAN in 2-methylbutane (2MB, Merck Uvasol grade) the temperature of which was slowly lowered from room level to a low value.

Results and Discussion

Let us first examine the suitability of the selected computational method for describing ESIPT in salicylic compounds (see Scheme 1). To this end, we shall check whether the first excited electronic states involved in the process (i.e., the enol, n, and keto structure, t, which correspond to the normal, nontransferred form, and the transferred form, respectively) are accurately positioned in energy terms and whether an energy barrier exists

TABLE 2: Structural Parameters for the Optimized Geometries of HBA in the Ground and Excited State as Calculated at B3LYP and TDDFT/B3LYP Levels with the TZVP Basis Set: Bond Lengths in Angstrom; Angles in Degrees

bond length/ angle	G.S. enol. symm C_s	first excited a (π,π^*) keto. symm C_1	first excited a″ (n,π^*) keto. symm C_s	first excited a″ (n,π^*) enol. symm C_s	gas-phase electron diffraction[47]
C1−C2	1.417	1.452	1.450	1.439	1.418 ± 0.014
C2−C3	1.405	1.378	1.417	1.431	
C3−C4	1.380	1.432	1.382	1.374	
C4−C10	1.401	1.370	1.389	1.402	
C9−C10	1.384	1.416	1.403	1.395	
C9−C1	1.397	1.418	1.384	1.383	
C2−C11	1.452	1.441	1.400	1.392	1.462 ± 0.011
C11−H12	1.105	1.084	1.081	1.097	
C1−O13	1.340	1.283	1.319	1.361	
C11−O14	1.228	1.315	1.340	1.306	1.225 ± 0.004
O13−H15	0.986	1.580	1.794	0.970	
O14−H15	1.760	1.029	0.976	1.877	
O13−O14	2.635	2.507	2.592	2.690	
C1−C2−C11−O14	0.0	14.9	0.0	0.0	
C1−C2−C11	120.3	118.3	121.2	121.0	121.5 ± 0.8
C2−C11−O14	124.4	120.9	126.9	126.6	123.8 ± 1.2
O14−C11−H12	119.6	116.1	112.3	112.6	119.7 ± 3.4
C1−C2−C3	119.4	118.9	117.0	117.7	118.2 ± 1.8

between the two. Then, we shall use the nature of the driving force controling the transformation to justify the substantial simultaneous increase in the acidity and basicity of the proton donor and acceptor, respectively, involved in the IMHB upon electronic excitation[31−33] in order to determine whether or not the process is feasible. Finally, we shall use these concepts to clarify the structural changes governing the photophysical behavior of HAN.

Suitability of the Computational Method Used. On the basis of the extensive available spectroscopic evidence,[34−39] we chose the two most simple salicylic compounds as models. Such compounds correspond to the structures with R = H (salicylaldehyde, HBA) and R = CH_3 (2-hydroxyacetophenone, HAP) in Scheme 1.

Salicylaldehyde. On the basis of available experimental evidence,[34−38] ESIPT in HBA involves a potential energy surface with a single minimum coinciding with the keto form; consequently, the proton transfer is subject to no energy barrier and the enol form is unstable. The situation in the ground electronic state is rather different, however. Thus, although the potential curve exhibits a single minimum, it falls in the region of the enol form.[32]

Theoretical descriptions of ESIPT processes are typically obtained with methods that include the effects of electronic correlations[32,40−44] (e.g., CASSCF methods in their CASPT2 and MRCI versions, the RI-CC2 method, and the DFT methods, all of which use optimized molecular geometries).

In 1999, Sobolewski and Domcke[45] studied HBA with molecular geometry optimization at the CASSCF level, using the 6-31G** basis set in conjunction with single-point calculations done with CASPT2. They assumed a C_s structure for the compound in all electronic states they examined and concluded that the ESIPT process was subject to no energy barrier and also that the keto form was the more stable, consistent with the experimental results. More recently, Aquino et al.[46] optimized the structure of HBA in various electronic states at the RI-CC2 and TDDFT levels, using the TZVP basis set and maintaining C_s symmetry. Their calculations confirmed that the ESIPT process in HBA is subject to no energy barrier and that the keto form is the more stable.

Our results at the TDDFT/B3LYP/TZVP level with no symmetry constraints on the molecular structure of HBA are consistent with those previously obtained by Sobolewski and Domcke[45] and Aquino et al.[46] and allow us to conclude that the keto form of the compound in its first $(\pi,\pi^*)^1$ state is a true energy minimum. However, the situation in the first $(n,\pi^*)^1$ state is different; in fact, both the enol form and the keto form are two energy minima, the former being more stable than the latter by about 2.9 kcal/mol. On the basis of the RI-CC2 calculations reported by Aquino et al.,[46] the keto structure of n,π^* nature should be at 3.19 eV (i.e., 3.38 eV below the corresponding (π,π^*) singlet) and HBA nonfluorescent as a result.

The calculated zero point energies (ZPEs) for the molecular structures corresponding to the energy minima allowed us to evaluate the 0−0 components of the corresponding electronic transitions between the two electronic states involved. Table 1 shows the most salient spectroscopic data obtained by Sobolewski and Domcke,[45] Aquino et al.,[46] and ourselves, together with their experimental counterparts where available. Note the good consistency between the theoretical (TDDFT/B3LYP//TZVP) calculations and the experimental spectroscopic values. Table 2 shows the experimental and theoretical values of the geometric parameters for the HBA structure. As can be seen, the B3LYP/TZVP calculations for this compound were quite good.

Figure 1 illustrates the energy variation of the molecular structures describing the proton transfer in the S_0 and S_1 (π,π^*) states of HBA. Following transfer, if the enol form of the compound in the ground state is electronically excited, the optimization process in the first $(\pi,\pi^*)^1$ excited state leads to the keto form, and any attempts at reaching the enol form fail. This is quite consistent with the above-described experimental photophysical behavior for the compound.

The enol form produced by electronic excitation of the compound is not an energy minimum (see Figure 1); therefore, its energy cannot be determined theoretically and nor can the stability gained by the keto form relative to the enol form by effect of the acidity and basicity changes that one can expect upon from electronic excitation. Lochbrunner et al.[16] recently recorded the photoelectron spectra for both tautomers of HBA in their excited electronic state as a function of the pump laser wavelength and pump−probe time delay. They used the onsets of the corresponding ionization bands to calculate the energy difference between the Franck−Condon structure for the excitation of the enol form and the keto form generated by proton transfer, which they found to be 0.5 eV; according to Weller,[31]

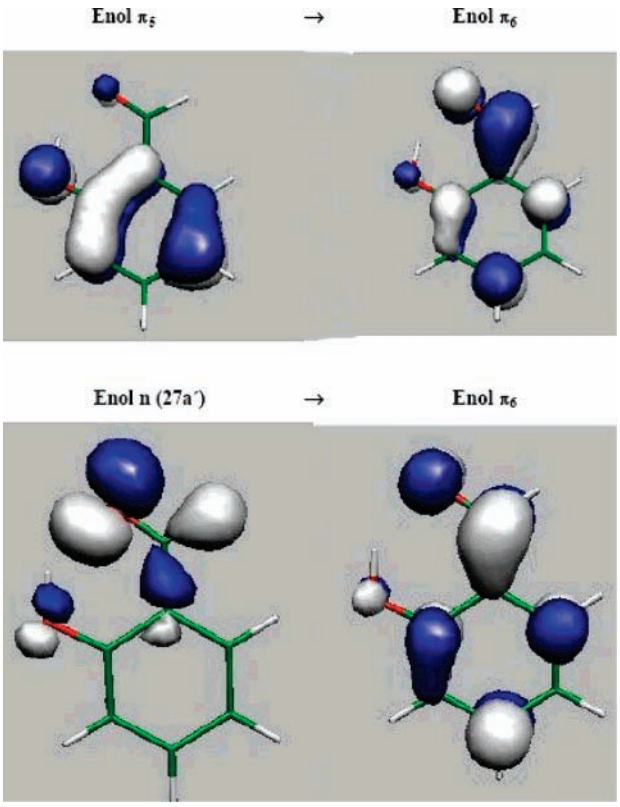

Figure 2. Molecular orbitals of HBA which characterize the electronic transitions $S_0 \rightarrow 1(\pi,\pi^*)^1$ and $S_0 \rightarrow (n, \pi^*)^1$ involved in the proton transfer from the enol form.

such strong stabilization must arise from deep acidity and basicity changes in the sites involved in the IMHB by effect of electronic excitation.

By using the same computational level for the doublets involved in the ionization of the enol and keto form, we found the latter to be 1.4 kcal/mol more stable than the former. Because the energy difference between vertical excitation is 9.84 kcal/mol greater in the enol form, the difference in ionization energy between the two forms is 11.2 kcal/mol (or 0.487 eV, which is quite consistent with the 0.5 eV obtained by Lochbrunner et al.[16]).

According to Weller,[31] the strong stabilization of the keto form relative to the enol form in the ESIPT process must arise from an increase in the acidity of its phenol group and the basicity of its carbonyl group, which form the IMHB, upon electronic excitation. On the basis of our calculations, the first $\pi \rightarrow \pi^*$ electronic transition is largely (94.5%) consistent with one between the HOMO and the LUMO. Figure 2 shows these molecular orbitals (enol π_5, π_6) for the enol form; as can be seen, electronic excitation strongly increases the acidity of the phenol group and the basicity of the carbonyl group, thereby favoring ESIPT and production of the keto form as a result. Let us examine the situation in the first (n,π^*) state in the light of these results. The reaction curve for the conversion of the electronically excited enol form (which is generated by excitation) to the keto form (which, as can be seen from Table 1, is 2.96 kcal/mol more stable) must be of the double-minimum type. What is thus the driving force for the process? Figure 2 shows the orbitals accounting for 97.5% of the electronic transition from n (27a′) to π_6 (6a″). Clearly, these MOs are incompatible with a substantial change in basicity or acidity, so the transformation process cannot be of the proton-transfer type; otherwise, it would involve the migration of a neutral proton from the phenol group to a half-occupied *n* MO in the carbonyl group.

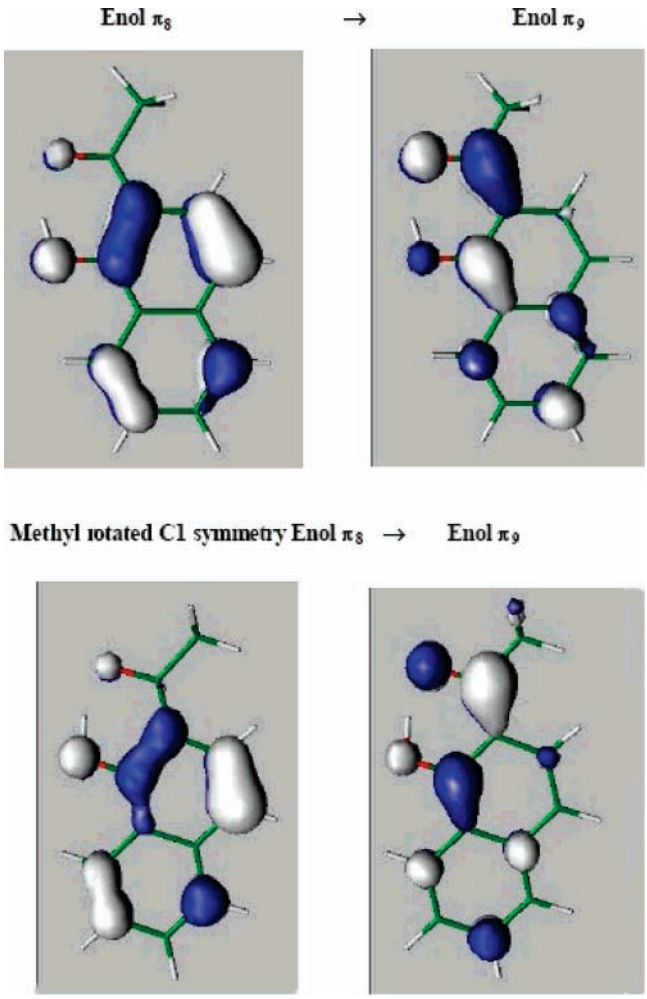

Figure 3. Molecular orbitals of HAN involved in the proton transfer from the enol form.

The similar results reached for HAP are reported as part of the Supporting Information.

On the Photophysics of HAN. We shall first examine the feasibility of the ESIPT process leading to the keto form of HAN upon electronic excitation of the enol form of the compound and then discuss various aspects of the photophysics of this compound outlined in the Introduction. Also, we will comment on the most recently reported theoretical data for the process.[48]

On the ESIPT Process. As shown above for HBA (Figure 2), the MOs of the Franck−Condon structure describing the $S_0 \leftrightarrow S_1$ electronic transition are consistent with a substantial change in acidity and basicity at the sites involved in the IMHB, which drive the ESIPT process in these compounds. However, the HOMO and LUMO of HAN (Figure 3), which account for 93.7% of such a transition, are suggestive of a change in acidity and basicity upon electronic excitation that is not strong enough to trigger a very fast proton transfer completing within 50 fs[16,17] and controlling its photophysics.

Recently, Szeghalmi et al.[7] computed the enol form of HAN in both the ground state and the first $(\pi,\pi^*)^1$ excited state at the CASSCF/6-31G(d,p) level by using an active space including the seven π orbitals and the first occupied σ orbital; also, they examined the photophysical behavior of the compound by Raman resonance spectroscopy. Their results warrant the

TABLE 3: Structural Parameters for the Ground State (GS) and Excited State of HAN as Calculated at the B3LYP and TDDFT/B3LYP Levels where Fully Optimized Geometries Were Obtained by Using the TZVP Basis Set: Bond Lengths in Angstrom; Angles in Degrees

bond length/ angle	CAS/ 6-31G(d,p)// $S_0(8,8)$[7]	CAS/ 6-31G(d,p)// $S_1(8,8)$[7]	GS enol C_s[a]	$1(\pi,\pi^*)^1$ enol C_1[b]	$1(\pi,\pi^*)^1$ E(Me[r]) C_1[c]	$1(\pi,\pi^*)^1$ keto C_1[d]	$1(n,\pi^*)^1$ enol C_s[e]	$1(n,\pi^*)^1$ enol C_s[f]	$1(n,\pi^*)^1$ keto C_1[g]
C1−C2	1.388	1.461	1.405	1.440	1.442	1.451	1.432	1.433	1.434
C2−C3	1.430	1.385	1.426	1.393	1.393	1.399	1.445	1.445	1.438
C3−C4	1.349	1.488	1.362	1.411	1.411	1.411	1.354	1.353	1.359
C4−C10	1.426	1.431	1.424	1.401	1.401	1.395	1.431	1.431	1.421
C10−C5	1.426	1.394	1.414	1.413	1.415	1.422	1.403	1.403	1.409
C5−C6	1.354	1.379	1.375	1.388	1.398	1.376	1.382	1.382	1.378
C6−C7	1.421	1.398	1.409	1.403	1.402	1.411	1.408	1.407	1.412
C7−C8	1.353	1.374	1.374	1.394	1.395	1.390	1.374	1.375	1.371
C8−C9	1.428	1.406	1.413	1.406	1.405	1.400	1.423	1.422	1.426
C9−C10	1.403	1.416	1.424	1.443	1.441	1.445	1.434	1.432	1.433
C9−C1	1.432	1.428	1.431	1.424	1.426	1.451	1.408	1.409	1.411
C2−C11	1.485	1.447	1.463	1.457	1.458	1.434	1.388	1.392	1.403
C11−C12	1.511	1.509	1.511	1.503	1.500	1.487	1.526	1.517	1.493
C1−O13	1.333	1.296	1.333	1.321	1.319	1.277	1.362	1.361	1.324
C11−O14	1.207	1.256	1.240	1.280	1.280	1.324	1.311	1.314	1.352
O13−H15	0.952	0.991	0.998	1.055	1.061	1.501	0.970	0.971	1.736
O14−H15	1.195	1.563	1.625	1.461	1.441	1.040	1.825	1.769	0.976
O13−O14	2.613	2.482	2.532	2.461	2.448	2.480	2.640	2.589	2.556
H−O−C−C			0.0	1.50	0.12	0.18	0.0	0.0	2.12

[a] Minimum, methyl 0.0°. Energy −613.620642, ZPE 0.190359 au. [b] Minimum, methyl 18.5°. Energy −613.497972, ZPE 0.184413 au. [c] Minimum, methyl 178.4°. Energy −613.497962, ZPE 0.184897 au. [d] Minimum methyl 175.3°. Energy −613.499327, ZPE 0.185139 au. [e] Minimum, methyl 0.0°. Energy −613.483438, ZPE 0.185595 au. [f] Minimum, methyl 180°. Energy −613.483868, ZPE 0.185517 au. [g] Minimum, methyl 10.5°. Energy −613.484416, ZPE 0.187152 au.

following conclusions: (a) theoretical and experimental displacement parameters were very highly consistent; (b) the vibrations exhibiting the highest shifts were those of stretching and in-plane deformation of the naphthalene ring and the conjugated carbonyl group where, by contrast, the OH stretching mode exhibited no appreciable enhancement; and (c) the MOs describing the $S_0 \leftrightarrow S_1$ transition were consistent with an even smaller increase in the basicity of the carbonyl group upon electronic excitation. These results further support the previous arguments that the ESIPT mechanism cannot occur so efficiently and rapidly upon electronic excitation as formerly assumed for this chromophore.

Surprisingly, optimization of the Franck−Condon structure generated by excitation of the stable enol form in the ground electronic state leads to an enol form with all-real numerical vibrational frequencies (i.e., to an energy minimum). The HOMO and LUMO of this molecular structure (Figure 3) are also consistent with the above-described slight increase in acidity and basicity upon electronic excitation. Thus, if the corresponding structure is generated with a transferred proton and C_1 symmetry, then geometry optimization leads to a keto form with the methyl group rotated by about 180° with respect to the situation in the ground state and having all-real vibrational frequencies (i.e., an energy minimum). We have thus identified two HAN forms in the first $(\pi,\pi^*)^1$ excited state that are true energy minima, one for the enol form and the other for the keto form. Although these forms are virtually degenerate in energy terms ($\Delta G = -0.39$ kcal/mol), on the basis of the above-described small changes in acidity and basicity, they cannot allow the enol form to be converted into the keto form in a rapid, complete manner.[17] We shall return to this point later on.

The dipolarity of the enol form of HAN increases upon electronic excitation to the first $(\pi,\pi^*)^1$ state (its dipole moment increases from 2.99 to 5.55 Debye); the corresponding keto form is slightly less polar (5.16 Debye). As can be seen from Figure 3, this transition clearly involves the unsubstituted benzene ring of the compound, which one should bear in mind in interpreting the disparate photophysical behavior of HAN relative to its monocyclic homolog HAP.

Table 3 shows the most salient geometric parameters for the previous molecular forms of HAN in its S_0 and S_1 states, the latter in both the enol form and keto form. As can be seen, the enol form changes markedly upon electronic excitation. Thus, the chelated cycle in HAN including the IMHB undergoes various changes the most important of which is that the distance between the phenolic hydrogen and the carbonyl proton is considerably shortened by effect of electronic excitation (from 1.625 Å in S_0 to 1.441 Å in S_1); by contrast, the distance between the oxygen atoms changes much less (from 2.532 Å in S_0 to 2.448 Å in S_1). Note the good consistency between the geometric parameters for HAN as determined at the TDDFT/B3LYP/TZVP level in this work and those obtained by Szeghalmi et al.[7] at the CASSCF/6-31G(d,p)//(8,8) level.

The presence of a stable enol form of HAN in its first $(\pi,\pi^*)^1$ state is consistent with the results obtained by Lochbrunner et al.[17] using Raman resonance spectroscopy in combination with transient absorption measurements with 30 fs time resolution, which led them to state that "no enhancement of the O−H stretch motions could be observed" and that "it shows that directly after the optical excitation, the hydrogen of the OH group is still bound to the oxygen, and does not directly move toward the oxygen of the aceto group as one might expect for an ESIPT molecule". This strengthens our arguments based on the anomalously small changes in the acidity of the phenol group and basicity of the carbonyl group observed upon electronic excitation in HAN. However, all this contradicts the assumption of Lochbrunner et al.[17] that the fluorescence emission of the compound originates from the keto form.

The facts that the enol form of HAN in its S_1 state has its methyl group in an eclipsed conformation with respect to the carbonyl oxygen, which coincides with the conformation in S_0, and that the keto form has its methyl group rotated by 180° with respect to the previous situation suggest that the excited enol form may initially undergo twisting of its methyl group in order to adopt a staggered conformation with respect to the

TABLE 4: Positions of the 0−0 Components for the Electronic Transitions of HAN as Calculated at the TDDFT/B3LYP//TZVP Level with Fully Optimized Geometries

	0−0 component	exptl
$S_0^n \rightarrow 1(\pi,\pi^*)^1_n$ methyl rotated 0°	390.6 nm	388.7 nm, ref 3
$S_0^n \rightarrow 1(\pi,\pi^*)^1_n$ methyl rotated 178°	389.0 nm	
$S_0^n \rightarrow 1(\pi,\pi^*)^1_t$ methyl rotated 180°	392.7 nm	
$S_0^n \rightarrow 1(n,\pi^*)^1_n$	344.0 nm	
$S_0^n \rightarrow 1(n,\pi^*)^1_t$	342.5 nm	

oxygen atom in the carbonyl group. Optimizing this conformation, which we name as E(Me^r) leads to an energy minimum with all-real frequencies and a free energy 0.3 kcal/mol higher than that of the normal enol form but retaining its dipolarity (viz. 5.59 Debye). Note that optimizing this structure in the ground state of the compound leads to no true energy minimum.

Table 3 shows the most salient geometric parameters for the new molecular structure E(Me^r). Worth special note are a very slightly lengthened OH bond (1.061 Å), a shortened distance between the carbonyl oxygen and the phenol hydrogen (1.441 Å), and an also shortened O−O distance (2.448 Å). As can be seen from the MOs of Figure 3, these results need not imply a change in the effects of electronic excitation on the acid−base properties of the molecule.

We located the first (n, π^*) singlets, both of which (enol and keto) were true energy minima and virtually isoenergetic (the keto form was only 0.5 kcal/mol more stable than the enol form) approximately 3200 cm^{-1} above the first (π,π^*) singlets. Table 3 shows the most salient geometric parameters for both structures. As can be seen, the IMHB was markedly weakened by effect of one of the highly localized electrons in the basic site being promoted to a π electron system. As a result, the distance between the phenolic proton and the carbonyl oxygen in the excited enol form increased from 1.441 Å in the $1(\pi,\pi^*)^1$ system to 1.825 in the $1(n,\pi^*)^1$ system, and so did the O−O distance (from 2.448 to 2.640 Å).

The fact that twisting about the methyl group generates two stable structures of very similar energies in the excited electron state of HAN is consistent with a mechanism allowing the transformation, within a few femtoseconds, of the enol form produced by electronic excitation; also, it provides an explanation for the doublet nature of the 0−0 component of the excitation of HAN under free-jet expansion conditions.[3]

The energies of the two structures involved in the temporal evolution of excited HAN were studied by Lochbrunner et al.[16] using time-resolved photoelectron spectroscopy. They found the splitting between the thresholds of the bands for the two structures to be 0.25 eV. Let us examine this evidence in the light of the structures present in the first excited electronic state of HAN from its most salient experimental and theoretical spectroscopic data (Table 4).

We have found that the doublet states involved in the ionization of the optimized enol and keto forms are true energy minima. Also, the doublet of the enol form is 1.37 kcal/mol more stable than that of the keto form; because the keto form is 5.48 kcal/mol more stable than the Franck−Condon structure of the enol form, the resulting splitting is 0.297 eV. The doublets for the enol form with a staggered methyl group have very similar energies, so the previous energy difference must be a result of that between the Franck−Condon structure of both enol forms, which is 4.62 kcal/mol in favor of the staggered form. The resulting splitting is therefore 0.200 eV. This value is consistent with the experimental splitting obtained by Lochbrunner et al.,[16] 0.25 eV, which suggests the occurrence

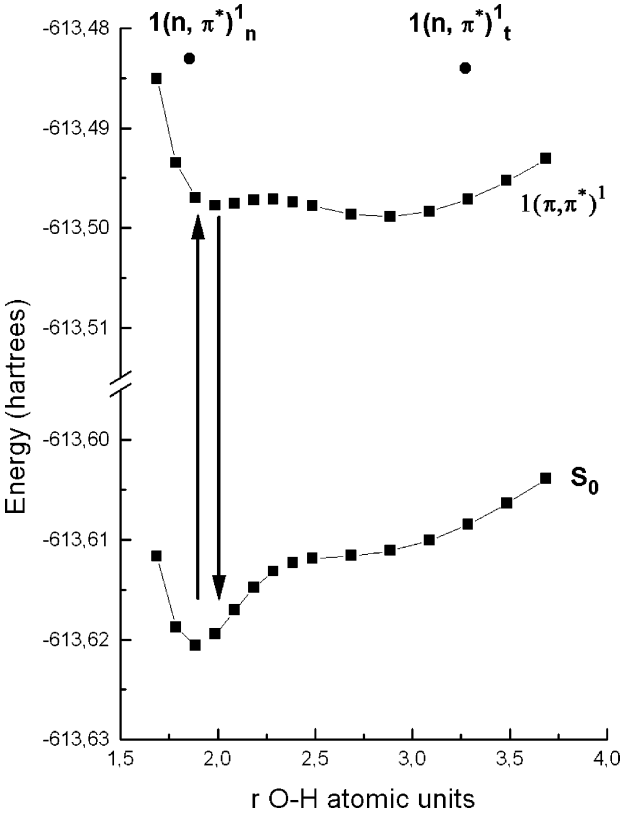

Figure 4. Potential energy profiles as a function of the donor O−H distance for the ground electronic state, S_0, and the S_1 (π,π^*) state of HAN as obtained by maintaining C_s symmetry. Stationary points were fully optimized under no symmetry constraint. All other points were calculated by freezing the O−H distance and fully optimizing the remaining geometrical parameters. The position of the $1(n,\pi^*)^1$ state is indicated.

of an ESIPT mechanism, twisting of the methyl group or both; the fact that twisting of the methyl group is consistent with the doublet nature of the excitation peaks of HAN, however, favors the torsional mechanism.

Figure 4 shows the PES for the S_0 and the S_1 (π,π^*) states of HAN as obtained by maintaining C_s symmetry. The enol form of S_1 (π,π^*) comprises two structures connected by twisting of the methyl group, which we name as E and E(Me^r) and possess about the same r_{OH} value; therefore, they cannot be distinguished in Figure 4, as well as the arrows indicating the absorption and emission processes, connected by twisting of the methyl group. Also, the absolute minima for the keto structure have the methyl group rotated by about 180° with respect to the ground state.

One other interesting notion in the photophysics of HAN is the so-called "trans-keto form" (see Scheme 2) proposed by Tobita et al.[8] to account for the transient absorption spectra obtained upon excitation of HAN to its first absorption bands (between 355 and 370 nm). According to these authors, the structure generated from the excited enol form becomes an excited structure, the precursor of the trans-keto form; such a structure rapidly falls to the ground electronic state via a radiationless mechanism and produces the trans-keto form, which is responsible for the transient absorption spectrum. Subsequently, Douhal et al.[6,10−15] hypothesized that the new HAN structure produced from the keto form, which they called KR*(276) (see Scheme 2), was stable and responsible for the peaks in what they called the "long wavelength fluorescence spectrum" for the compound.

Surprisingly, optimization at the TDDFT level of the excited electronic state of KR*(276) led to no energy minimum but

rather to a structure that reconverted into an energy minimum in the ground electronic state (see KROH in Scheme 2). Such a structure, however, departed from that typical of the compound in the ground state, which is the enol form. On the basis of the electronic transitions of this structure, it exhibits a first singlet at 404 nm that coincides with the maximum of the first band in the transient absorption spectrum for HAN in cyclohexane at 293 K obtained by Tobita et al.,[8] a second singlet at 373 nm that falls within such a band, and a third and fourth singlet at 291 and 283 nm, respectively, which coincide with the second band in the transient absorption spectrum. It should be noted that these bands may result from proton transfer to the carbonyl group and the resulting torsion in the hydroxyl group but not from twisting about the C−C bond which connects the aceto group to the ring as proposed by Douhal et al.;[6,10−15] in fact, judging from the MOs involved in the electronic excitation, twisting must be hindered by the increased double character of the bond. Also, the structure proposed by Tobita et al.[8] (see Scheme 2) is inconsistent with the measured transient absorption spectrum, the first two calculated singlets for which appear at 379 and 373 nm, respectively.

While this paper was being refereed, a new study on the HAN molecule was reported by Ortiz-Sánchez et al.[48] These authors also examined the intramolecular excited-state proton transfer of HAN at the DFT level but employed the 6-31G** basis set instead. They concluded that the $1(\pi,\pi^*)^1$ state in both the enol and the keto form is a true minimum, the keto form being 0.52 kcal/mol more stable and the energy barrier between the two being 0.27 kcal/mol. Also, they found the keto form to be unstable in the ground state, as was previously inferred from calculations at the MP2 level.[5] Then, the potential energy curve for the proton transfer in the ground electronic state exhibits a single minimum at the enol structure. These authors also found KR* type structures, which they had previously processed at the CIS/HF level,[6,10−15] to be significantly more unstable than the keto structure (K*), so they cannot be used to account for the photophysics of HAN. Hence, the results published in reference 48, though fragmentary, are consistent with those examined in this work.

Absorption and Emission of HAN. The first band in the UV−vis absorption spectrum or dissolved HAN at 298 K is an isolate band between 420 and 320 nm that is scarcely sensitive to the polarity of the medium; in fact, the only change from cyclohexane to DMSO to the gas phase (at 368 K) is that the maximum shifts from 366 to 367 to 358 nm. Also, depending on the particular solvent, the onset of the band is at 410−420 nm, and only a shoulder is observed at approximately 380 nm.[2] Under free-jet expansion conditions, the 0−0 component is at 388.7 nm and shifts to 387.0 nm upon deuteration of the OH group.[3]

Table 4 shows the theoretical values of the 0−0 components computed in this work. The 0−0 component of the $S_0^n \leftrightarrow S_1^n$ transition is predicted to fall at 390.6 nm and that for deuterated HAN is predicted at 389.1 nm. The calculated energies of the 0−0 components for the three most important structures of HAN in the first π,π^* excited electronic state are so close to one another that both the rotated enol form and the keto form are consistent with the experimentally determined splitting in the 0−0 component under free-jet conditions (see Table 4). However, nonverticality in the transition between the enol form in S_0 and the excited keto form (with respect to twisting of the methyl group in the enol form) must be negligible; therefore, the origin must be the two enol forms present in S_1.

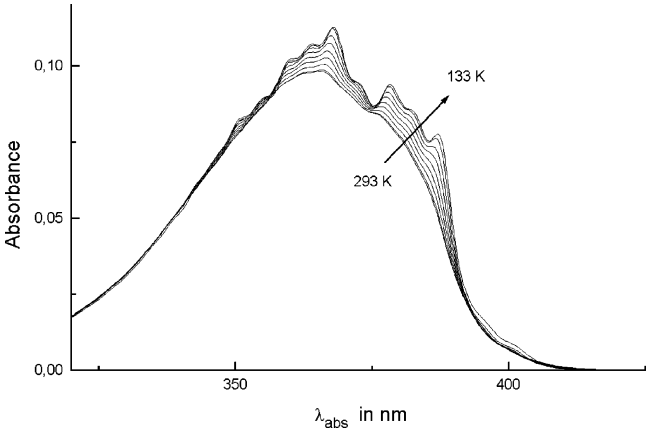

Figure 5. UV−visible absorption spectra for a 10^{-5} M solution of HAN in 2-methylbutane at temperatures from 293 to 133 K as corrected for volume reduction as the temperature was lowered.

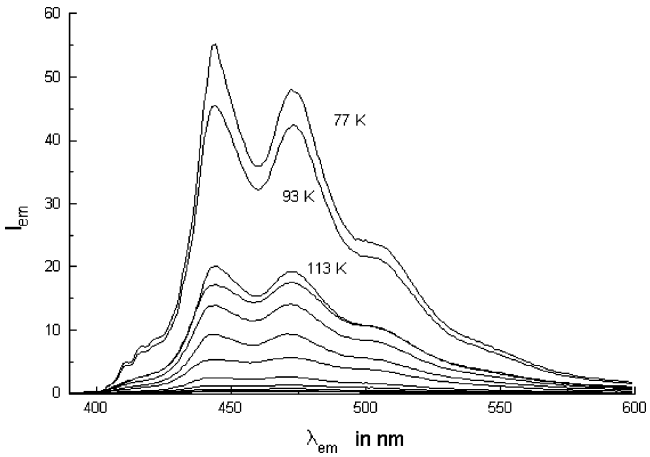

Figure 6. Emission spectra for 10^{-5} M HAN in 2-methylbutane obtained at temperatures from 293 to 77 K. $\lambda_{exc} = 340$ nm.

The increased structuring in the fluorescence band for dissolved HAN at a low temperature has been used to account for the involvement of various forms present in S_1.[12] We therefore thought it of interest to examine the behavior of a diluted solution of HAN in such an inert solvent as 2-methylbutane as the solution temperature was lowered.

Figure 5 shows the first UV−vis absorption band for a 10^{-5} M solution of HAN in 2MB over the temperature range 292−313 K, throughout which the solvent remained liquid. Lowering the solution temperature increased band structure and the absorbances in the 385 and 365 nm regions. Also, it resulted in structuring in the onset of the band at approximately 400 nm and in a negligible bathochromic shift in the band.

Figure 6 shows the fluorescence spectra for the previous solution over the temperature range 293−77 K. These spectra warrant some interesting comments, namely: (a) The fluorescence quantum yield increased significantly with decreasing temperature while the solution remained liquid (e.g., 58 times from 293 to 133 K) but soared when the solution solidified and the spectroscopic matrix for 2MB was formed as a result (see Figure 6). (b) The envelope of the fluorescence bands retained its shape to the extent that the spectra were superimposable. (c) The emission intensity concentrated around two maxima at 444 and 473 nm. (d) As in the absorption spectrum (Figure 5), the low-energy region was structured at the lowest temperatures studied.

The emissive behavior of HAN also warrants several interesting comments, namely: (a) The marked increase in emission

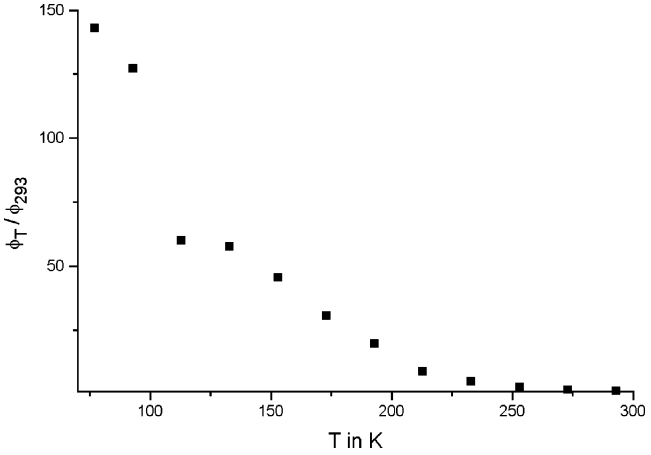

Figure 7. Variation of the emission quantum yield of HAN in 2-methylbutane at temperatures from 293 to 77 K with respect to that at 293 K.

intensity at a constant absorbance (Figure 7) clearly indicates that the viscosity of the medium delays a radiationless pathway allowing dissipation of the emission of the compound. This is the origin of the dramatically increased intensity when the medium becomes rigid (i.e., below the melting point of 2-methylbutane). Obviously, such a radiationless pathway must produce of a nonplanar structure of HAN, most probably through dramatic deformation of the planarity of the chelate bearing the IMHB.

(b) As the previous pathway is delayed, the form producing the deformed structure is lost to a lesser extent, so any emission from it will increase its contribution. The fact that the spectral envelope was not affected by the temperature suggests that HAN emits largely via a single structure (either the enol[2] or keto form[6]) or three,[3] in the latter case. However, the three structures would have to be connected via extremely fast equilibria for the contributions of their emissions to remain constant at any temperature.

(c) If one compares the absorption and emission of HAN in 2-methylbutane at 293 K (Figure 8a) with those at 77 K (Figure 8b) in an appropriate manner[49] in order to identify any mirror symmetry between the two and uses the absorption spectrum to superimpose the spectral envelope corresponding to a situation of mirror symmetry in the emission, the two are found to be very similar. This allows one to conclude the following: (1) the emitting molecular structure is very similar to the absorbing structure (i.e., to the enol form in the ground electronic state, which is the only structure present in the ground state of HAN). This excludes the possibility of HAN emitting largely from the excited keto form as proposed by Lochbrunner et al.[16] (2) The likeness between the mirror image of the emission spectrum and the absorption spectrum for the compound (see Figure 8) is inconsistent with the assumption of Douhal et al.[3] that the initial portion of the spectrum corresponds to emission from the enol form and that the strong peaks at 444 and 473 nm can be assigned to the origins of the emissions from the keto and KR*276 forms; in fact, such peaks are already present in the absorption spectra recorded at low temperatures, so they must be produced by something very similar to the excited enol form of the compound.

(d) On the basis of the low-temperature absorption and emission spectra (Figures 5, 6, and 8), the 0−0 component of HAN in 2-methylbutane (2MB) lies in the 403 nm region.

Photophysics of HAN. On the basis of the foregoing, we can rationalize the photophysics of HAN by using the molecular

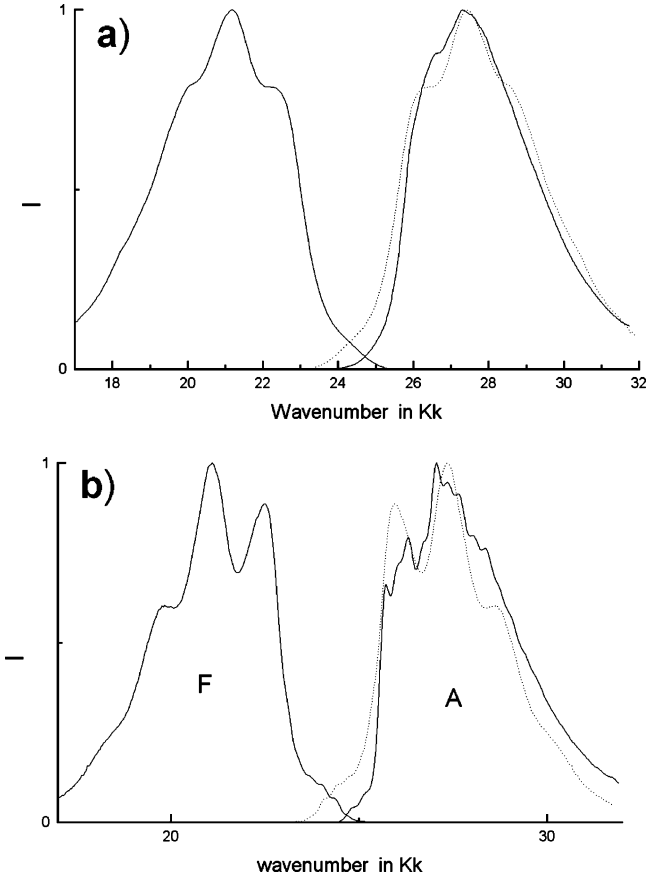

Figure 8. Analysis of the potential mirror-image symmetry between the first absorption and the fluorescence bands of HAN at 293 K (a) and 77 K (b) following appropriate correction.[49]

diagram of Figure 9. Excitation of the stable form in the ground electronic state of the compound (viz., its enol form) produces a stable enol form that emits via the minimum in the S_0 state (the emission can thus be structured) and becomes an enol form with its methyl group staggered with respect to its carbonyl oxygen. This new molecular form of HAN is also emissive and its emission structured in theory. The presence of these degenerate structures provides an explanation for the fact that, under free-jet conditions,[3] the 0−0 component of the $S_0 \rightarrow S_1$ transition splits into a doublet as spectral resolution is raised. This new enol form may also generate the corresponding keto form by proton transfer or an alternative form with a strongly deformed chelate ring; this latter form would be unstable and return to the ground electronic state, where it would adopt a structure consistent with the transient absorption observed by Tobita et al.[8] Our diagram invalidates that used by Douhal et al.[4] to account for the photophysics of HAN as regards not only the ground electronic state, S_0, but also the first $(\pi,\pi^*)^1$ excited state. The recent theoretical results of Ortiz-Sánchez[48] contradict the model of Douhal et al.[4] not only because they exclude the presence of a $1(\pi,\pi^*)^1$ state with two minima separated by a substantial energy barrier in the proton-transfer energy curve,[4] but also because they confirm that the only stable structure which can be reached in the ground state is the enol form[5] and that using the presence of the KR* structures in the excited state to explain the fluorescence of HAN is unwarranted as such structures lie about 11.1 kcal/mol above the excited-state enol−keto forms. Because the electronically excited enol forms cause no substantial change in acidity or basicity, they cannot be the driving forces dictating the photophysics of HAN via an ESIPT process leading to the corresponding keto form. In addition, a

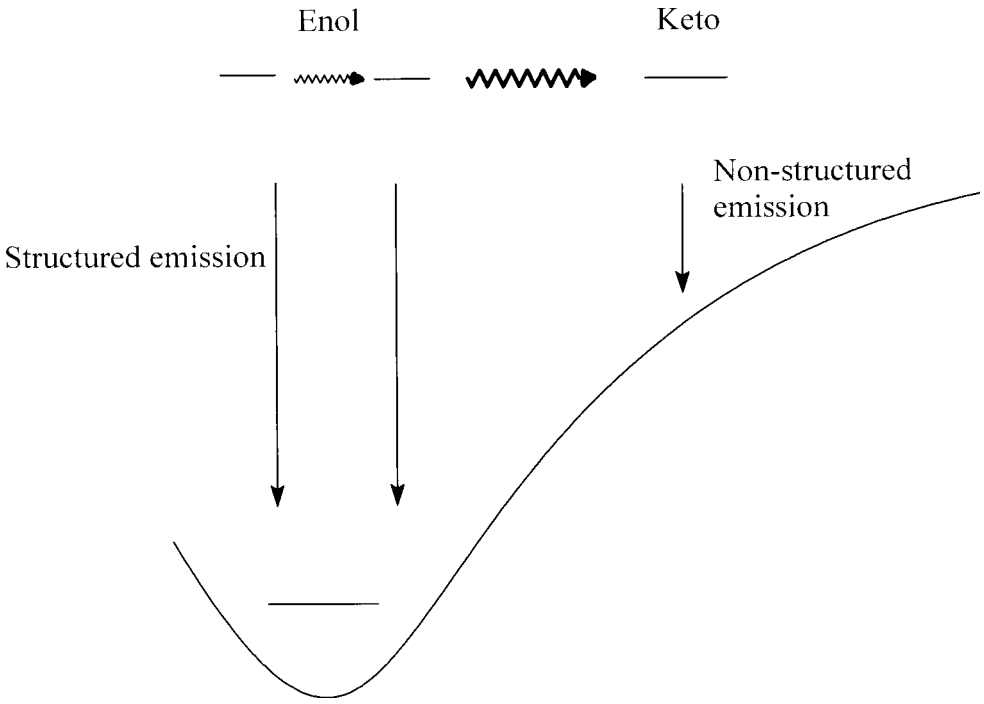

Figure 9. Outline of the proposed photophysics for HAN.

potential emission from the keto form would lie in the repulsive region of the proton-transfer curve for the ground electronic state (Figure 9) and thus be structureless.

The fast potential equilibrium between the two excited enol forms is consistent with the fact that the spectral envelope of HAN is temperature-independent. The variation of the emission quantum yield as the temperature is lowered suggests the presence of an efficient energy dissipation mechanism potentially related to the photostability of the compound and hence that, as noted earlier, it occurs in its enol form.[3,50]

The photophysical scheme proposed by Ortiz-Sánchez et al.[48] to explain the photophysics of HAN as a result of an ultrafast photoproton transfer between the enol and the keto forms in the excited electronic state fails to account for major experimental evidence. Thus, it does not explain why the peaks in the spectra for HAN at a low temperature in the gas phase are split into doublets[3] since such doublets must have resulted from the allowed enol → enol* Franck−Condon transition and from a highly unlikely enol → keto* nonvertical transition. Also, their model fails to explain the increased fluorescence quantum yield and the fact that, as shown in this work, the fluorescence envelope remains virtually unchanged as the temperature of a dilute solution of HAN in such an inert solvent as 2MB is lowered. Finally, their model provides no explanation for the facts the HAN emission exhibits neither vibronic structure nor mirror symmetry with its absorption at both room temperature and 77 K.

Conclusions

HAN exhibits two stable enol forms in its first $(\pi,\pi^*)^1$ electronic excited state that can easily reconvert by twisting about their methyl group. The presence of these two excited enol forms at very similar energy levels is consistent with the singular photophysical features of this compound (e.g., the split doublets in the fluorescence excitation spectra obtained under free-jet conditions or its femtosecond time-resolved photoelectron spectrum).

The diagram put forward by Douhal et al.[4] to explain the photophysics of HAN is inaccurate as regards the ground electronic state and the first (π,π^*) excited singlet.

The anomalous increase in the emission quantum yield of a 10^{-5} M solution of HAN in 2MB as the temperature is lowered suggests the presence of an effective radiationless mechanism accounting for the high photostability of the enol forms of the compound.

Acknowledgment. The authors are grateful to Spain's Dirección General de Investigación Cientifica y Técnica (DGICYT) for funding Project No. CTQ2005-03052 and also to the CCC of UAM for providing computer time.

Supporting Information Available: Structural parameters, calculated spectroscopic data, molecular orbitals of HAP involved in proton transfer from the enol form. This material is available free of charge via the Internet at http://pubs.acs.org.

References and Notes

(1) Catalán, J.; del Valle, J. C. In *14th Symposium on Photochemistry*; K.U. Leuven, Belgium, 1992; p 163.
(2) Catalán, J.; del Valle, J. C. *J. Am. Chem. Soc.* **1993**, *115*, 4321.
(3) Douhal, A.; Lamani, F.; Zehnacker-Rentien, A. *Chem. Phys.* **1993**, *178*, 493.
(4) Douhal, A.; Lahmani, F.; Zewail, A. H. *Chem. Phys.* **1996**, *207*, 47.
(5) Catalán, J.; Palomar, J.; De Paz, J. L. G. *Chem. Phys. Lett.* **1997**, *269*, 151.
(6) Organero, J. A.; García-Ochoa, I.; Moreno, M.; Lluch, J. M.; Santos, L.; Douhal, A. *Chem. Phys. Lett.* **2000**, *328*, 83.
(7) Szeghalmi, A. V.; Engel, V.; Zgierski, M. Z.; Popp, J.; Schmitt, M. J. *Raman Spectrosc.* **2006**, *37*, 148.
(8) Tobita, S.; Yamamoto, M.; Kurahayashi, N.; Ysukagosi, R.; Nakamura, Y.; Shizuka, H. *J. Phys. Chem. A* **1998**, *102*, 5206.
(9) Lu, C.; Hsieh, R. M.; Lee, I. R.; Cheng, P. Y. *Chem. Phys. Lett.* **1999**, *310*, 103.
(10) Organero, J. A.; Moreno, M.; Sants, L.; Lluch, J. M.; Douhal, A. *J. Phys. Chem. A* **2000**, *104*, 8424.
(11) Organero, J. A.; Tormo, L.; Douhal, A. *Chem. Phys. Lett.* **2002**, *363*, 409.
(12) Organero, J. A.; Santos, L.; Douhal, A. In *Femtochemistry and Femtobiology: Ultrafast Dynamics in Molecular Science;* Douhal, A., Santamaría, J., Eds.; World Scientific: Singapore, 2002; p 225.
(13) Organero, J. A.; Douhal, A. *Chem. Phys. Lett.* **2003**, *373*, 426.
(14) .Organero, J. A.; Douhal, A. *Chem. Phys. Lett.* **2003**, *381*, 759.
(15) Douhal, A. *Acc. Chem. Res.* **2004**, *37*, 349.

(16) Lochbrunner S.; Schultz, T.; Schmitt, M.; Shaffer, J. P.; Zgierski, M. Z.; Stolow, A. *J. Chem. Phys.* **2001**, *114*, 2519.
(17) Lochbrunner, S.; Szeghalmi, A.; Stock, K.; Schmitt, M. *J. Chem. Phys.* **2005**, *122*, 244315.
(18) Ahlrichs, R; Bär, M.; Häser, M.; Horn, H.; Kölmel, C. *Chem. Phys. Lett*. **1989**, *162*, 165. See http://www.turbomole.com. At present, TURBOMOLE is developed and supported by COSMOlogic GmbH & Co., K.G., Germany.
(19) Becke, A. D. *Phys. Rev. A* **1988**, *38*(6), 3098.
(20) Becke, A. D. *J. Chem. Phys.* **1993**, *98*, 5648.
(21) Lee, C.; Yang, W.; Parr, R. G. *Phys. Rev. B* **1988**, *37*, 785.
(22) Ahlrichs, R.; Furche, F.; Grimme, S. *Chem. Phys. Lett.* **2000**, *325*, 317.
(23) Schäfer, A.; Huber, C.; Ahlrichs, R. *J. Chem. Phys.* **1984**, *100*, 5829.
(24) Weigend, F.; Ahlrichs, R. *Phys. Chem. Chem. Phys.* **2005**, *7*, 3297.
(25) Casida, M. E. Time-Dependent Density Functional Response Theory for Molecules. In *Recent advances in density functional methods*, Part I; Chong, D. P., Ed.; World Scientific Press: Singapore, 1995; pp 155−193.
(26) Furche, F. *J. Chem. Phys.* **2001**, *114*, 5982.
(27) Furche, F.; Ahlrichs, R. *J. Chem. Phys.* **2002**, *117*, 7433.
(28) Furche, F.; Ahlrichs, R. *J. Chem. Phys.* **2004**, *121*, 12772.
(29) Furche, F.; Rappoport, D. Density Functional Methods for Excited States: Equilibrium Structure and Electronic Spectra. In *Computational Photochemistry*, Vol. 16 of Computational and Theoretical Chemistry; Olivucci, M., Ed.; Elsevier: Amsterdam, 2005; pp 93−128.
(30) Rappoport, D.; Furche, F. *J. Am. Chem. Soc.* **2004**, *126*, 1277.
(31) Weller, A. Z. *Elektrochem* **2004**, *60*, 1144.
(32) Catalán, J.; Palomar, J.; de Paz, J. L. G. *J. Phys. Chem. A* **1997**, *101*, 7914.
(33) Catalán, J. *J. Am. Chem. Soc.* **2001**, *123*, 11940.
(34) Catalán J.; Toribio, F.; Acuña, A. U. *J. Phys. Chem.* **1982**, *86*, 303.
(35) Nagaoka, S.; Nagashima, U. *Chem. Phys.* **1989**, *139*, 153.
(36) Nagaoka, S.; Hirota, N.; Sumitani, M.; Yoshihara, K.; Lipczynska-Kochany, E.; Iwamura, H. *J. Am. Chem. Soc*. **1984**, *106*, 6913.
(37) Morgan, M. A.; Orton, E.; Pimentel, G. C. *J. Phys. Chem.* **1990**, *94*, 7927.
(38) Nishiya, T.; Yamauchi, S.; Hirita, N.; Baba, M.; Hanozaki, I. *J. Phys. Chem*. **1986**, *90*, 5730.
(39) Orton, E.; Morgan, M. A.; Pimentel, G. C. *J. Phys. Chem.* **1990**, *94*, 7936.
(40) Sobolewski, A. L.; Domcke, W. *Chem. Phys.* **1984**, *184*, 115.
(41) Luth, K.; Scheiner, S. *J. Phys. Chem.* **1994**, *98*, 3582.
(42) Hass, K. C.; Schneider, W. F.; Stévez, C. M.; Bach, R. D. *Chem. Phys. Lett*. **1996**, *263*, 414.
(43) Sobolwski, A. L.; Domcke, W. *Chem. Phys.* **1998**, *232*, 257.
(44) Sobolewski, A. L.; Domcke, W. *Chem. Phys. Lett*. **1999**, *300*, 533.
(45) Sobolewski, A. L.; Domcke, W. *Phys. Chem. Chem. Phys.* **1999**, *1*, 3065.
(46) Aquino, A. J. A.; Lischka, H.; Hättig, C. *J. Phys. Chem. A* **2005**, *109*, 3201.
(47) Borisenko, K. B.; Bock, C. W.; Hargittai, I. *J. Phys. Chem.* **1996**, *100*, 7426.
(48) Ortiz-Sánchez, J. M.; Gelabert, R.; Moreno, M.; Lluch, J. M. *J. Chem. Phys.* **2007**, *127*, 084318.
(49) Birks, J. B.; Dyson, D. J. *Proc. Roy. Soc. A* **1963**, *275*, 135.
(50) Catalán, J.; Fabero, F.; Guijarro, M. S.; Claramunt, R. M.; Santa María, J. D.; Foces-Foces, M. C.; Cano, F. H.; Elguero, J.; Sastre, R. *J. Am. Chem. Soc.* **1990**, *12*, 747.